Available online http://amq.aiqua.it
ISSN (print): 2279-7327, ISSN (online): 2279-7335

Alpine and Mediterranean Quaternary, 33 (2), 2020, 165-181 https://doi.org/10.26382/AMQ.2020.12

THE EARLY HOLOCENE BUCHWIESE ROCK AVALANCHE (EASTERN ALPS, AUSTRIA): GEOLOGICAL CONDITIONS, KINEMATICS, MORPHOLOGICAL AND SEDIMENTARY LEGACY.

Jürgen M. Reitner [1], Susan Ivy-Ochs [2], Olivia Steinemann [2], Daniela Lattner [3], Alexander Römer [1]

[1] Geologische Bundesanstalt / Geological Survey of Austria, Vienna, Austria.
[2] Laboratory of Ion Beam Physics, ETH Zurich, Zurich, Switzerland.
[3] Former member of the Geological Survey of Austria, Vienna, Austria.

Corresponding author: J.M. Reitner <juergen.reitner@geologie.ac.at>

ABSTRACT: In this study we reconstructed the Buchwiese rock avalanche in the Lienz Dolomites in Eastern Tyrol (Austria). We used a multi-method approach combining geological field mapping, the analysis of digital elevation model (DEM) data, cosmogenic ^{36}Cl exposure dating, and a geoelectrical survey to unravel the detachment mechanisms, emplacement processes and timing of the Buchwiese rock avalanche. According to the results of the ^{36}Cl exposure dating, the event took place at 10.8±0.9 ka during the Early Holocene. The failure of a rock mass with a volume of $27x10^6$ m^3 was enabled by a dip-slope in strata of the Kössen Formation (limestone, marls, claystone), Oberrhätkalk (massive to thickly bedded limestone), Allgäu Formation (mottled limestone and marl) and Rotkalk (red nodular limestone and marl), in combination with N-S to NNE-SSW trending brittle faults. We regard fatigue of the fine-grained rocks of the Kössen Fm. (claystone, marl), typical slaking rocks, since the Last Glacial Maximum as the major cause for this catastrophic rock slope failure. With the reconstructed drop height (H) of 1200 m and runout length (L) of 3.5 km, the Buchwiese rock avalanche has a Fahrböschung angle α of 19° and H/L ratio of 0.36. Due to the geological conditions, the initial failure occurred as a plane slide. In the deposition area, we observe strong control of lithological properties, topographic conditions, and substrate materials along the pathway on the morphology and sedimentology of the rock avalanche deposit. Longitudinal ridges, indicating spreading of an unconfined flow, are comprised mostly of massive limestone (Oberrhätkalk). The carapace facies consisting of clast-supported boulders is only developed in areas with limestone (mostly Oberrhätkalk but also limestone of the Kössen Fm.). The body facies in the upper parts are dominated by jigsaw subfacies with a subordinate occurrence of fragmented subfacies in the outcrops. Even in the middle part of the deposition area, we observe the prevalence of the moderately fragmented jigsaw subfacies within large areas of Kössen Fm. debris, which consists of alternating claystone, limestone beds. Such a finding may indicate preferential deformation within the claystone beds. After partial collision with a bedrock ridge and a small jump, the fragmented subfacies dominates. This collision led to the formation of a fan-like megaboulder cluster consisting of detached and fragmented Oberrhätkalk boulders with volumes up to 1000 m^3 and a fan-like distribution. The results of geoelectrical surveys reflect different amounts of fragmentation with the carapace facies, showing high resistivity, while the body facies reveals low resistivity. Preserved source stratigraphy within the dilated rock mass indicates predominantly laminar rock avalanche movement. All the morphological and sedimentary evidence supports a dynamic fragmentation model as the best mechanical explanation for the Buchwiese rock avalanche.

Keywords: Rock avalanche, fragmentation, cosmogenic ^{36}Cl exposure dating, Holocene, Eastern Alps.

1. INTRODUCTION

Large catastrophic rock slope failures (rock slides, rock avalanches) with volumes of >10^6 m^3 are rare but are nevertheless perhaps the most spectacular forms of mass displacement in high-relief mountains (Abele, 1974). They suddenly change landscapes and have been perceived in human history as catastrophes. Due to the usually surprising occurrence of such rapid landslides, the enormous amount of energy released as a result and corresponding dust formation, there are no direct observations of the processes like internal and basal facies fragmentation (Hewitt et al., 2008). Our understanding of catastrophic rock slope failures, their mechanics and kinematics, mostly relies on the study of paleo-events and thus on the morphological and geological legacy of such processes (Heim, 1932; Abele, 1974; Erismann & Abele, 2001).

Among these catastrophic rock slope failures, rock avalanches are the most fascinating features due to high velocities of more than 200 km/h and due to an extremely long runout (Heim, 1932; Abele, 1974; Hewitt et al., 2008). The comprehension of how rock is transformed to a highly fragmented material that acts like a laminar fluid with reduced friction is one of the great challenges in landslide research (Hungr et al., 2005; Davies & McSaveney, 2009; Imre et al., 2010; Aaron & McDougall, 2019). Thus, the description of lithological properties of original and crushed bedrock may, together with that of morphological features, provide a sound basis for a better understanding of the processes involved (Dunning, 2004; Crosta et al., 2007; Weidinger et al., 2014; Dufresne et al.; 2016a, b; Dufresne & Dunning, 2017) and for modelling approaches (e.g.

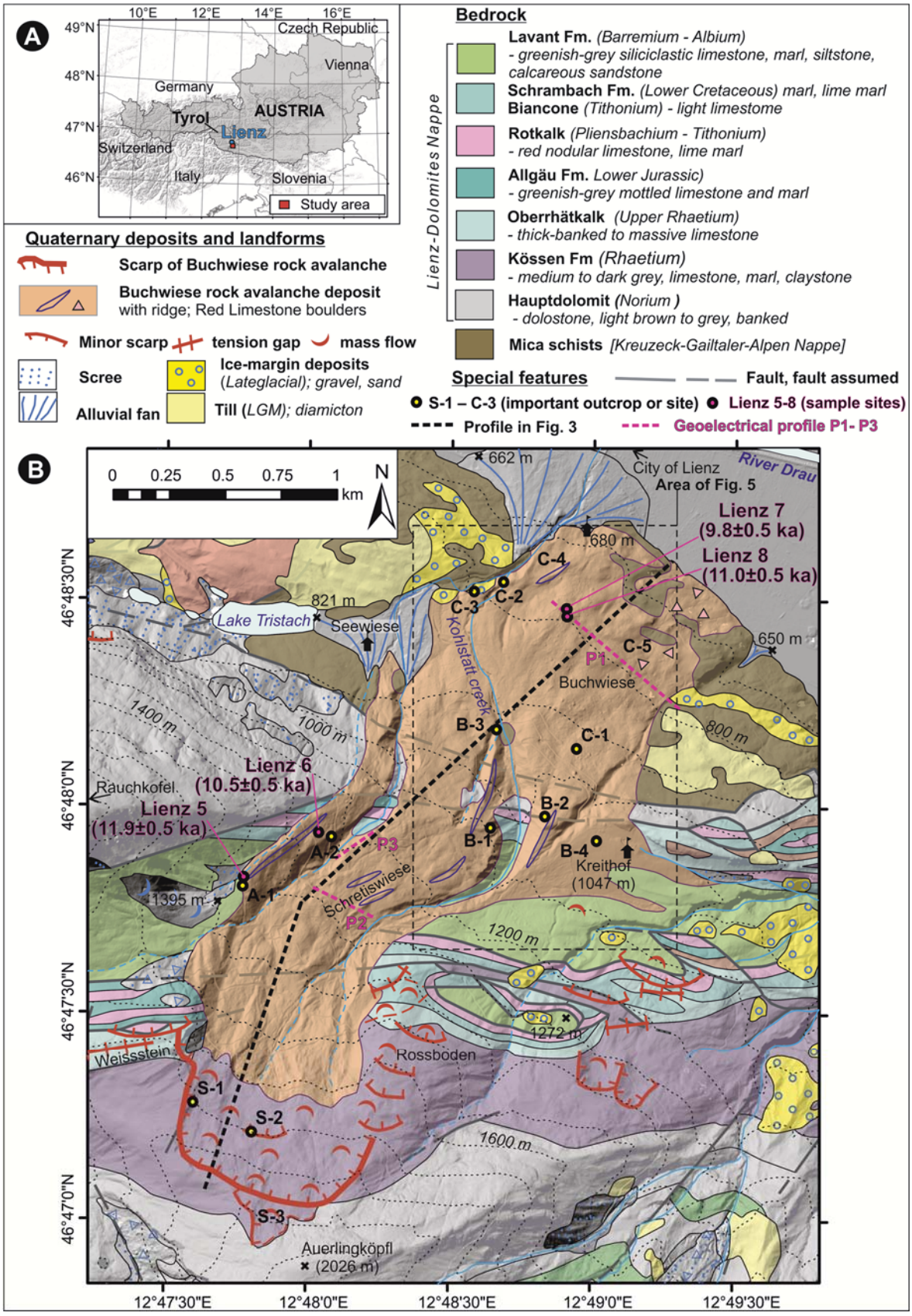
A
10°E
12°E
14°E
16°E
49°N
48°N
47°N
46°N
Czech Republic
Vienna
Germany
AUSTRIA
Tyrol
Lienz
Switzerland
Italy
Slovenia
Study area
Bedrock
Lienz-Dolomites Nappe
Lavant Fm. (Barremium - Albium)
- greenish-grey siliciclastic limestone, marl, siltstone, calcareous sandstone
Schrambach Fm. (Lower Cretaceous) marl, lime marl
Biancone (Tithonium) - light limestome
Rotkalk (Pliensbachium - Tithonium)
- red nodular limestone, lime marl
Allgäu Fm. Lower Jurassic)
- greenish-grey mottled limestone and marl
Oberrhätkalk (Upper Rhaetium)
- thick-banked to massive limestone
Kössen Fm (Rhaetium)
- medium to dark grey, limestone, marl, claystone
Hauptdolomit (Norium)
- dolostone, light brown to grey, banked
Mica schists [Kreuzeck-Gailtaler-Alpen Nappe]
Quaternary deposits and landforms
Scarp of Buchwiese rock avalanche
Buchwiese rock avalanche deposit
with ridge; Red Limestone boulders
Minor scarp
tension gap
mass flow
Scree
Ice-margin deposits
(Lateglacial); gravel, sand
Alluvial fan
Till (LGM); diamicton
Special features
Fault, fault assumed
S-1 – C-3 (important outcrop or site)
Lienz 5-8 (sample sites)
Profile in Fig. 3
Geoelectrical profile P1- P3
B
0
0.25
0.5
0.75
1
km
N
662 m
City of Lienz
Area of Fig. 5
River Drau
Lienz 7
(9.8±0.5 ka)
Lienz 8
(11.0±0.5 ka)
680 m
C-4
C-2
C-3
821 m
Lake Tristach
Seewiese
Kohlstatt creek
P1
C-5
650 m
Buchwiese
1400 m
1000 m
B-3
C-1
800 m
Lienz 6
(10.5±0.5 ka)
Rauchkofel
Lienz 5
(11.9±0.5 ka)
B-2
B-1
A-2
R3
B-4
Kreithof
(1047 m)
1395 m
A-1
Schreliswiese
P2
1200 m
1272 m
Weissstein
Rossboden
S-1
S-2
1600 m
S-3
Auerlingköpfl
(2026 m)
46°48'30"N
46°48'0"N
46°47'30"N
46°47'0"N
12°47'30"E
12°48'0"E
12°48'30"E
12°49'0"E
12°49'30"E

Aaron et al., 2020; Singeisen et al., 2020). In addition, there is great societal interest, especially in countries with increasingly populated Alpine valleys, in the potential danger related to such rapid landslides. Hence, a better perception of causes and triggers of such hazards ranging e.g. from material fatigue, over earthquakes to climate change and, finally, of the chronology of processes before the failure are of eminent importance (e.g. Eisbacher & Clague, 1984; Zerathe et al., 2014; Wood et al., 2015). Recent progress in geochronology, especially the application of surface exposure dating with terrestrial cosmogenic nuclides like ^{10}Be and ^{36}Cl (Ivy-Ochs & Kober, 2008) together with ^{14}C and U/Th dating (Prager et al., 2008; Ostermann et al., 2007, 2017) is enabling a tremendous extension of the dated paleolandslide record in the Alps (Prager et al., 2008; Ivy-Ochs et al., 2017; Pánek, 2019).

Bauer (1990) first mentioned a rock avalanche deposit in the study area. Reitner (2003a) provided a first detailed map and description of the Buchwiese rock avalanche with an estimated volume of c. 22x10^6 m^3. In this paper, we present new geological, geochronological and geophysical data of the reconstructed pre-historical Buchwiese rock avalanche, as a contribution to research on catastrophic landslides in the Alps. The aim of this study is to show the influence of different lithologies and thus rock properties together with that of topographic conditions and substrate materials along the pathway on the morphology and sedimentology of the rock avalanche deposit.

2. GEOLOGICAL SETTING AND PREVIOUS RESEARCH

The study area is located in Eastern Tyrol on the northern flank of the Lienz Dolomites mountain group within the Eastern Alps, c. 5 km SE of the city of Lienz in the Drau Valley (Fig. 1, 2). Tectonically, the Lienz Dolomites mountain group is part of the Austroalpine Superunit and, more specifically, of the Drauzug-Gurktal Nappe System (Schmid et al., 2004; Schuster et al., 2014). The latter is subdivided in the study area into the Lienz-Dolomites Nappe and the Kreuzeck-Gailtaler-Alpen Nappe (Linner et al., 2013).

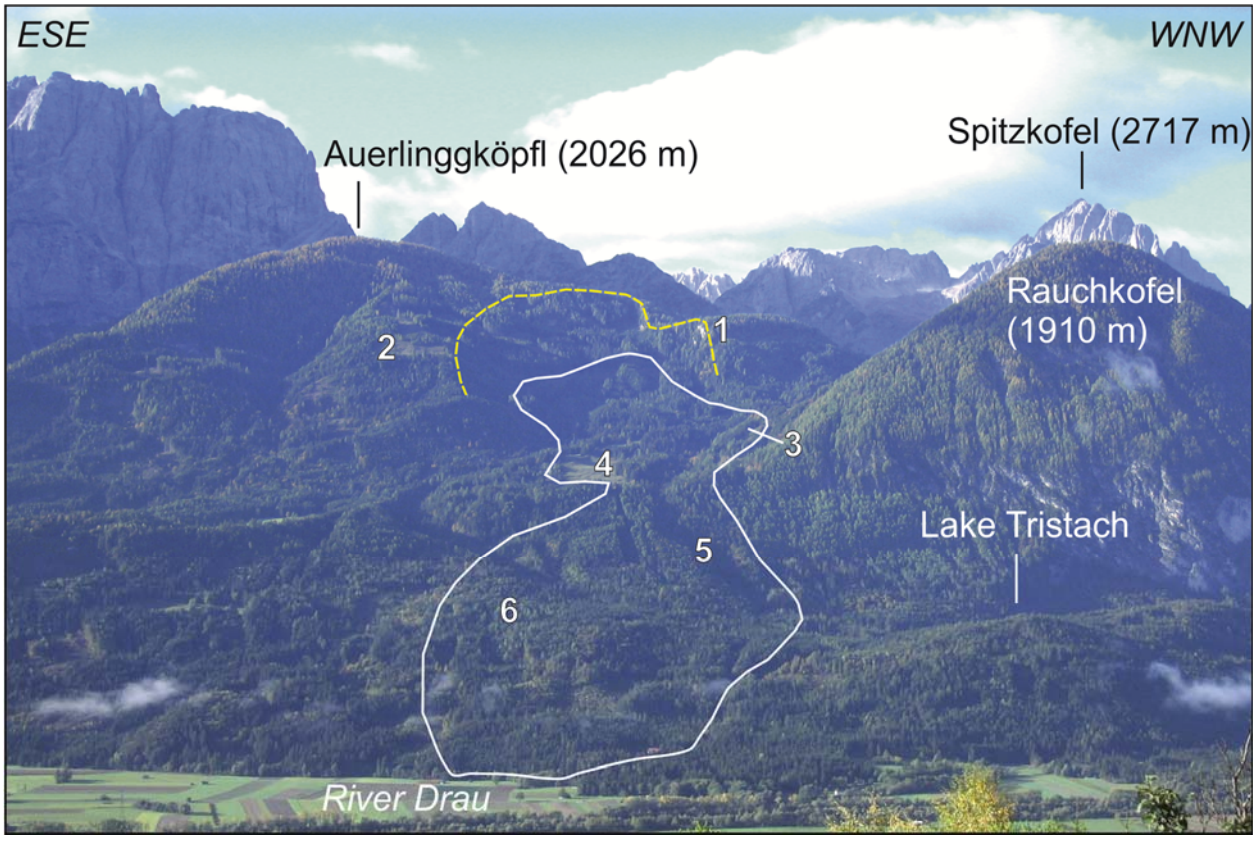

Fig. 2 - View from the opposite Drau Valley flank on the study area and surrounding. The yellow steepled line shows the run of the scarp of the Buchwiese rock avalanche followed by the deposition area surrounded by the white line. Note the subglacially shaped peaks like Rauchkofel and Auerlingköpl in contrast to the rugged peaks above like Spitzkofel indicating nunataks during the LGM. Numbers indicate following locations: 1 - Weissstein, 2 - Rossboden, 3 - longitudinal ridge with boulders Lienz 5 and Lienz 6, 4 - Kreithof, 5 - Kohlstatt creek, 6 - Buchwiese.

<<< ---------- ----------

Fig. 1 - Maps showing (a) the location of the study area and (b) the geology (modified after Linner et al., 2013). Contour interval is 100 m. The bold steepled black line shows the traces of the geological profile in Fig. 3.

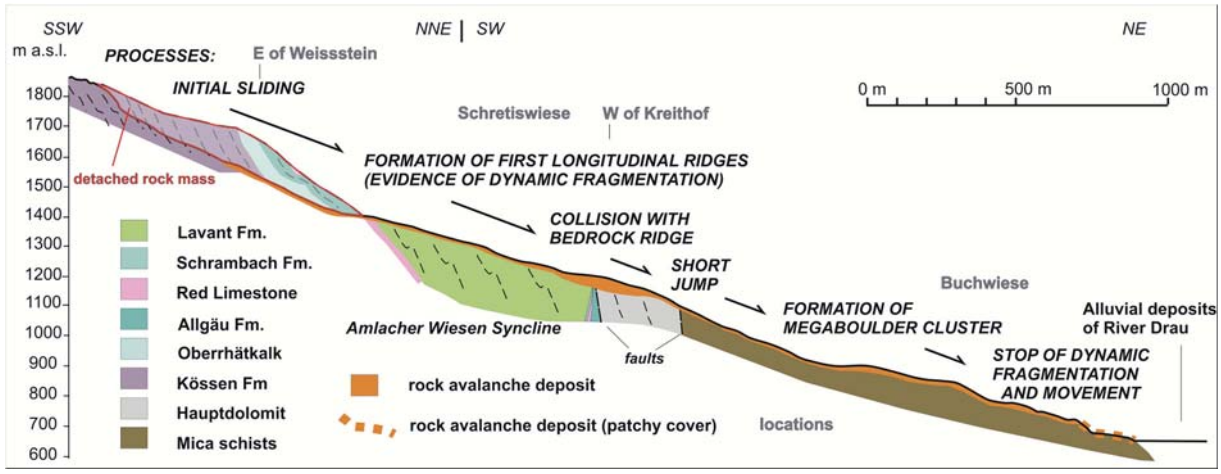

Fig. 3 - Geological profile of the rock avalanche area and the sequence of processes during rock avalanche formation and emplacement (for location see Fig. 1).

The source area and the upper and middle part of the deposition area of the Buchwiese rock avalanche are made up of rocks of the tectonically higher Lienz-Dolomites Nappe (Figs. 1, 3), which occur in the Amlacher Wiese Syncline (Schmidt, 1995; Blau & Grün, 1995). The lowermost part of the deposition area is underlain by mica schists of the Kreuzeck-Gailtaler-Alpen Nappe. Descriptions of fault systems and their chronology are provided by Schmidt (1995), Brandner et al. (2001) and, in combination with a hydrogeological characterisation of faults and rocks, by Probst et al. (2003).

The scarp area is part of the southern limb of the Amlacher Wiesen Syncline with a general dip towards the north. In the following, the lithology of the rocks in the scarp area are characterised according Bauer (1990):

- The Kössen Formation (Rhätium) in the study area consists of an interbedded up to 350 m thick sequence of black pelites (claystone, marls) and dark limestone with an ochre colour due to weathering (Fig. 4a). Geotechnically, the fine-grained lithologies (claystone and marl) are classified as slaking rocks showing disintegration upon exposure to air or moisture in combination with an irreversible loss of strength (Fig. 4b). A large number of mass movements, mostly slides and mass flows, in the Northern Calcareous Alps in Tyrol and Bavaria are linked with the occurrence of this lithology (Nickmann, 2009; Nickmann & Thuro, 2013; Lotter & Gruber 2020). Even moderate weathering is sufficient for reaching the critical state for failure (Nickmann & Thuro, 2013), and in a dip-slope setting the saturated Kössen Fm. tends to fail at slope angles of 10-15° (Lotter & Gruber, 2020).
- The Oberrhätkalk on top of the Kössen Fm. consists mostly of massive but sometimes thickly bedded limestone with a thickness of up to 25 m (Fig. 4c). This brittle lithology makes up cliffs, like Weissstein (Figs. 1, 2) or bedrock ridges, like north of Kreithof (Fig. 5).
- The Allgäu Formation (Lower Jurassic) in the scarp area consists of greenish-grey mottled limestone and marls, partly chert-bearing. The marls are also classified as slaking rocks. Rotkalk (red nodular limestone and marl; Pliensbachium - Tithonium) has a thickness of 7 to 17 m (Blau & Grün, 1995).

During the Last Glacial Maximum (LGM; = Würmian Pleniglacial) the area was covered by the Drau Glacier, which was part of the large Alpine transection glacier complex (Reitner et al., 2016). The ice surface was in the range of 2200 m a.s.l. (Reitner, 2003b) with only the highest sharp peaks (Fig. 2) as nunataks above. Subglacial till consisting of a matrix-supported and massive diamicton showing a high consolidation is typical of temperate glaciers of the LGM (Reitner & Menzies, 2020). Glacial erosion is evident in the overdeepened Lienz Basin with a maximum bedrock depth of c. 600 m below the valley floor just north of the study area (Burschil et al., 2019). Additional documents of subglacial shaping are the mica schist areas within the small

---------- ----->>>>>

Fig. 4 - Images from the field in the scarp (S) area and in the uppermost deposition area (A) : 4a) Outcrop S-1 (for location see Fig. 1) with the typical appearance of the nortward dipping Kössen Fm. as an alternation of limestone, marl and claystone beds (1m scale). 4b) Close up of claystone showing a disintegration typical for slaking rock (1m scale). 4c) view from east towards the Weissstein consisting of massive to thickly bedded Oberrhätkalk limestone. 4d) Subordinate scarp at S-2 with the northward dipping Kössen Fm (dip 360/56) in a typical dip-slope situation. Note encircled person for scale. 4e) The boulder Lienz 5 consisting of massive Oberrhätkalk limestone sampled for ^{36}Cl exposure dating at the outer flank of uppermost longitudinal ridge. Note the rounded edges. 4f) Outcrop A-1 at the same ridge as Lienz-5 (in Fig. 4e) showing clast supported diamicton (lithofacies SCc) with very angular Oberrhätkalk clasts. Note the whitish colour of the surface due a thin, very bright, floury, calcareous precipitation (Image: B. Imre). 4g) Outcrop A-2 with jigsaw facies within Oberrhätkalk (1m scale). 4h) Outcrop A-2 with fragmented facies consisting of a diamicton with very angular clasts of the Kössen Fm. limestone (1m scale) (Image: B. Imre).

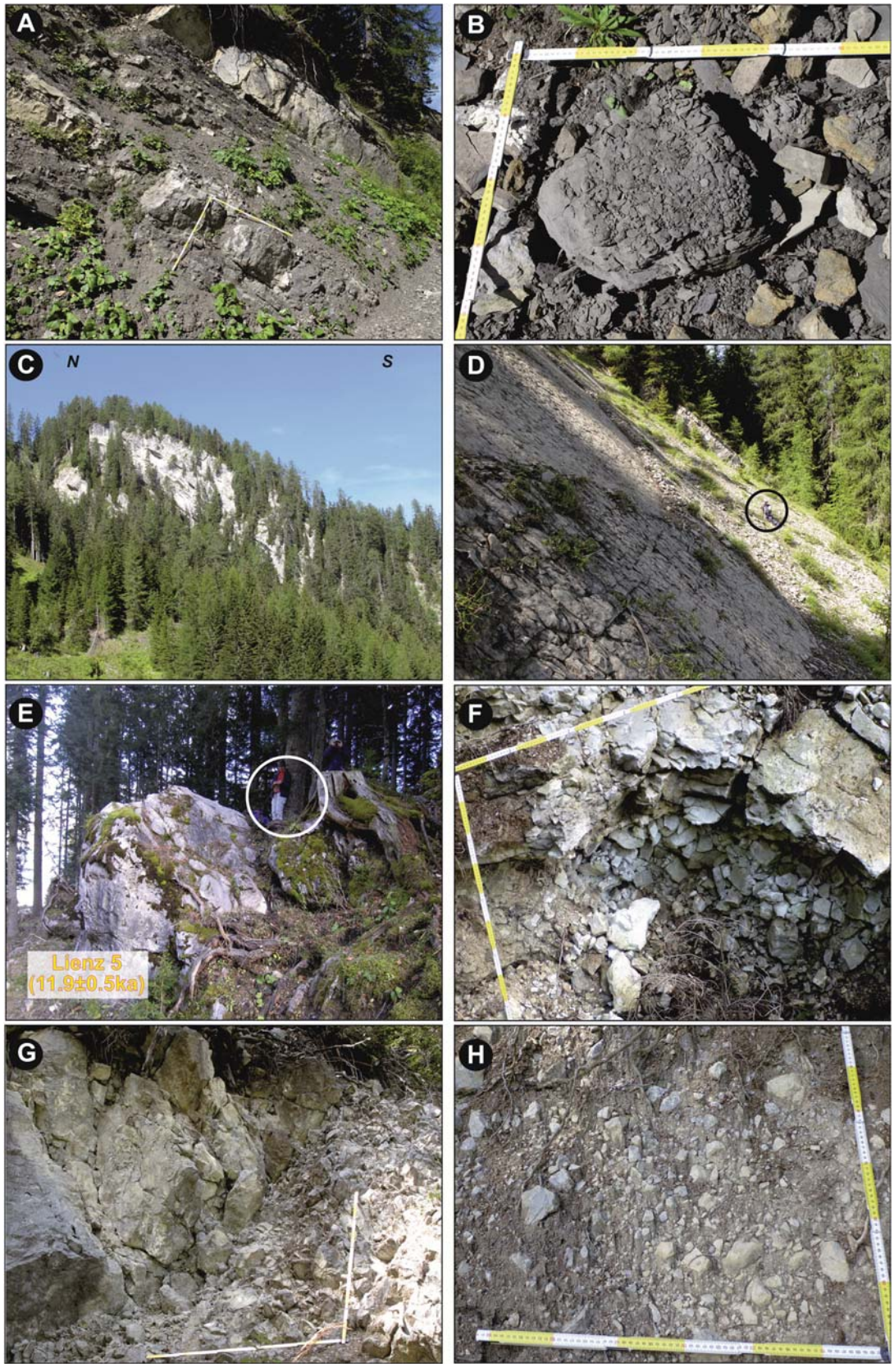
A
B
C
N
S
D
E
Lienz 5
(11.9±0.5ka)
F
G
H

basin of Lake Tristach (Fig.1) as well as rounded peaks like the Rauchkofel (Fig. 2) and the abraded bedrock ridge north of Kreithof (Fig. 5).

Following the climax of the LGM (27-19 ka; Monegato et al., 2007; Ivy-Ochs, 2015), remnants of delta deposits document the brief early Lateglacial phase of ice-decay (~19 ka) in the study area (Reitner et al., 2016). By 18.5 ka the glacier tongue area (Schmidt et al., 2002) and all major Alpine valleys (van Husen, 2000), like the Drau Valley at Lienz, were free of ice. Afterwards no Lateglacial advances affected the study area. The following phase was characterised by infill of the overdeepened basin (Burschill et al., 2019) and by fluvial erosion. On the surrounding slopes, different types of mass movements occurred ranging from deep-seated slope deformations to rock slides and rock avalanches (Bauer, 1990; Reitner, 2003 a, b; Reitner et al., 2014; Reitner & Linner, 2009). The area of Lienz has low seismicity (cf. Reiter et al., 2018) with no faults known to be tectonically active.

3. METHODS

Geological mapping at the 1:10,000 scale was performed in the year 2000 (Reitner, 2003a) for the Geological map sheet Lienz (Linner et al., 2013). Further morphological analysis of the mostly forested terrain benefitted from available high-resolution airborne laser scanning data and a digital elevation model (DEM) with 1-m resolution, which were provided by TIRIS (www.tirol.gv.at/) since 2010. For lithofacies descriptions, we applied the coding of Keller (1996). We performed landslide volume estimations by reconstructing a pre-failure surface of the scarp area and calculating the differential volume of this surface and the present surface (DEM) in ARCMAP. 2.5-dimensional models were produced using ARCSCENE.

We took four samples from the tops of the largest boulders in the Buchwiese rock avalanche deposit for cosmogenic ^{36}Cl surface exposure dating in November 2007. All sampled boulders are of Oberrhätkalk limestone. Sample information is given in Tab. 1. Sample preparation followed the method of isotope dilution (^{35}Cl) described in Ivy-Ochs et al. (2004). Total Cl and ^{36}Cl were measured in the same target at the ETH accelerator mass spectrometry (AMS) facility of the Laboratory for Ion Beam Physics (LIP) with the 6 MV tandem. Measured ^{36}Cl/Cl ratios were normalized to the ETH internal standard K382/4N with a value of ^{36}Cl/Cl =17.36×10^{-12}, which is calibrated against the primary ^{36}Cl standard KNSTD5000 (Vockenhuber et al., 2019). Measured ratios were corrected for a full process chemistry blank value of 4.2±3.6×10^{-15}. We calculated ^{36}Cl exposure ages with the LIP ETH in-house MATLAB

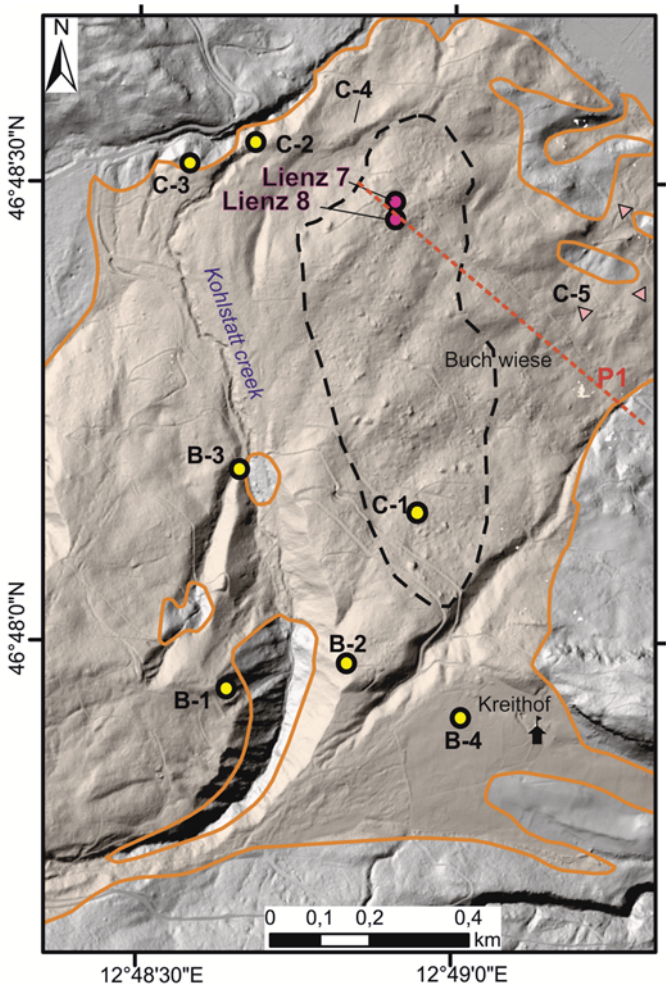

Fig. 5 - DEM showing characteristic morphological elements in the lower part of the deposition areas B and C. The most striking features are the bedrock ridge north of Kreithof, the fan-like morphology SW of Kreithof and the megaboulder cluster surrounded by a black steepled line. The rock avalanche deposit is indicated in orange. Pink triangles show the cluster of Rotkalk boulder. The red line shows the run of the geoelectrical profile P1.

Sample	Latitude	Longitude	Elevation	Boulder size (LxWxH)	Sample thickness	Shielding	^{36}Cl concentration[a,b]	Cl	Exposure age no erosion correction[c]	Exposure ages 5 mm/ka erosion[c]
			m a.s.l.	m	cm		10^6 at/g_{rock}	ppm	ka	ka
Lienz 5	46.797.102	12.796.282	1372	4x4x4	3.5	0.9615	0.735 ± 0.022	15.12 ± 0.25	11.5 ± 0.5	11.9 ± 0.5
Lienz 6	46.798.889	12.800.654	1257	4x3x1.5	3.5	0.9567	0.602 ± 0.019	17.53 ± 0.2	10.2 ± 0.5	10.5 ± 0.5
Lienz 7	46.807.975	12.815.125	790	4x4x3	5	0.97878	0.398 ± 0.015	15.72 ± 0.23	9.5 ± 0.5	9.8 ± 0.5
Lienz 8	46.807.657	12.815.141	804	4x4x3	3.5	0.97878	0.426 ± 0.016	14.10 ± 0.28	10.7 ± 0.5	11 ± 0.5

[a] Measured against standard K382/4N, (17.36 (± 0.35) × 10^{-12}), which is calibrated to the primary standard KNSTD5000 (Christl et al., 2013; Vockenhuber et al., 2019).
[b] Corrected for processed blank of (4.2 ± 3.6) × 10^{-15} ^{36}Cl/^{35}Cl.
[c] Production rates as in Alfimov & Ivy-Ochs (2009) and references therein (Sp_{Ca} 48.8 ± 3.4 at/g_{Ca}/a). Rock density of 2.4 g/cm^3 was used.

Tab. 1 - Sample information and results of ^{36}Cl surface exposure dating.

Sample	Al_2O_3 %	CaO %	Fe_2O_3 %	K_2O %	MgO %	MnO %	Na_2O %	P_2O_5 %	SiO_2 %	TiO_2 %	Sm ppm	U ppm	Th ppm
Lienz 5	0.24	55.5	0.1	0.06	0.67	<0.01	0.2	<0.01	0.44	<0.01	0.4	1.35	0.05
Lienz 6	0.3	55.7	0.11	0.09	0.67	<0.01	0.1	0.06	0.67	0.01	0.1	0.55	0.05
Lienz 7	0.15	56.7	0.15	0.06	0.3	<0.01	<0.1	<0.01	0.34	<0.01	0.1	0.55	0.05
Lienz 8	0.15	53.4	0.09	0.05	0.63	0.01	<0.1	<0.01	0.32	<0.01	0.1	0.55	0.05

Tab. 2 - Elemental composition of leached samples. Values below detection limit are marked with "<". Cl values are from AMS measurements.

code based on the parameters presented in Alfimov & Ivy-Ochs (2009 and references therein) and the elemental composition of every rock sample (measured with ICP-MS at Act labs S.A., Ontario, Canada) (Tab. 2). Ages have been corrected for topographic shielding, which was measured in the field using compass and clinometer. Shielding corrections were calculated with the topographic shielding calculator in the online calculator at https://hess.ess.washington.edu. Ages were corrected using an erosion rate of 5 mm/ka (André, 2002). No correction was made for snow cover; in general, such corrections are made only on bedrock samples (cf. Bichler et al., 2016). Final errors on the ages (Tab.1) include both analytical and production rate uncertainties.

We performed a geoelectrical survey to foster a 2D -image of the rock avalanche structure. Landslide investigations with the integration of geoelectrical outcomes for landslide characterization, like description of landslide geometry body, can be found in Perrone et al. (2004) and a comparable case study about rock avalanche deposit in Ostermann et al. (2012). A good overview about theory and field design and the limitations of the resistivity method is given in Aizebeokhai (2010) and Loke et al. (2013). Three electrical resistivity tomography (ERT) profiles (P1, P2, P3; location indicated in Fig. 1) were carried out in August 2012 with a GEOMON4D resistivity meter, an in-house development of the Geological Survey of Austria. 93 electrodes were used with the specific layout parameters listed in Tab. 3. For better resolution, we used a gradient electrode array configuration (Dahlin & Bing, 2006) with 4300 measurements. Power input of electrical current was adequate (100-400 mA) and data quality was quite good. Sample analysis showed, that electrical noise was sufficiently low and occasional 50 Hz crosstalk could be eliminated with sufficient time window length. Geoelectrical processing started with raw data filtering, like elimination of outliers, analysis of signal to noise ratio, etc. Geoelectrical inversion was carried out with the Res2DInv software (©Geotomo Software, Malaysia). Following standard procedures, we inverted geoelectrical data with a smooth inversion based on an L2-norm criterion, with an average resistivity starting model and topographic correction incorporated into the inversion (Loke, 2019).

4. RESULTS

4.1 Field description

In order to facilitate the field description, the area is subdivided into four domains: Scarp area and the deposition areas A-C (from proximal to distal, see Fig. 1).

Scarp area

The maximum 800 m wide and 0.7 km^2 large detachment niche lies between the limestone bedrock ridge of Weissstein (Fig. 4c) in the west and the Rossboden in the east (Fig. 2). In the uppermost detachment area between 1700 m and 1900 m a.s.l., the niche diminishes successively in the upward direction indicating in total a missing rock mass (Fig. 3). The majortiy of the detachment niche is made up of Kössen Fm. which shows a general dip towards north. Dip angles are in the range of 30 to 50° but may vary due to small scale folding between 30° towards south and 75° towards north. Given the original slope at Weissstein with angle of 37° (Fig. 3), a dip-slope situation is evident as indicated by large outcrops (S-1, S-2; Figs. 1, 4a, 4d). In addition, still ongoing creep movement in the average 25° steep terrain results in an undulating surface (Fig. 1), proof of the weak rock mechanical properties of the Kössen Fm. (claystone, marls). This is also visible in tension gaps and small scarps at the eastern margin of the scarp area. The Weissstein is made up of up to 25 m thick Oberrhätkalk (Figs. 2, 4c), which is overlain on the northern flank by folded dark Allgäu Fm. and up to 15 m of Rotkalk (Figs. 1, 3). The southern margin of the detachment area north of Auerlingköpfl peak (2026 m a.s.l.) consists of Hauptdolomit (thick-bedded, bench-forming dolostone). The presence of large dolostone boulders indicates loosening of Hauptdolomit after the detachment of the rock mass consisting of Kössen Fm. at this location.

N-S to NNE-SSW oriented segments of the western scarp mirror rare minor near vertical brittle faults (at S-1in Fig. 1). Such a direction is also evident in the joint distribution of the outcrops and as well in lineaments (Fig. 1) in the areas consisting of brittle Hauptdolomit.

Deposition area A (Schrettiswiese)

Just 600 m downslope of the limestone cliff of Weissstein, a prominent SW-NE trending ridge marks the lateral limit of the rock avalanche deposit. This 350 m long ridge consists on the surface of large limestone boulders of Oberrhätkalk (Fig. 4e). The height on its outer side is around 5 m. Based on the incised creek which did not reach bedrock, the thickness of the rock avalanche deposit is most likely in the range between 20 and 60 m.

Electrical tomography profile	Unit electrode spacing [m]	Length [m]	Orientation
Buchwiese P1	10	760	NW-SE
Buchwiese P2	4	304	WNW-ESE
Buchwiese P3	3	228	SW-NE

Tab. 3 - Key parameters of the electrical tomography profiles.

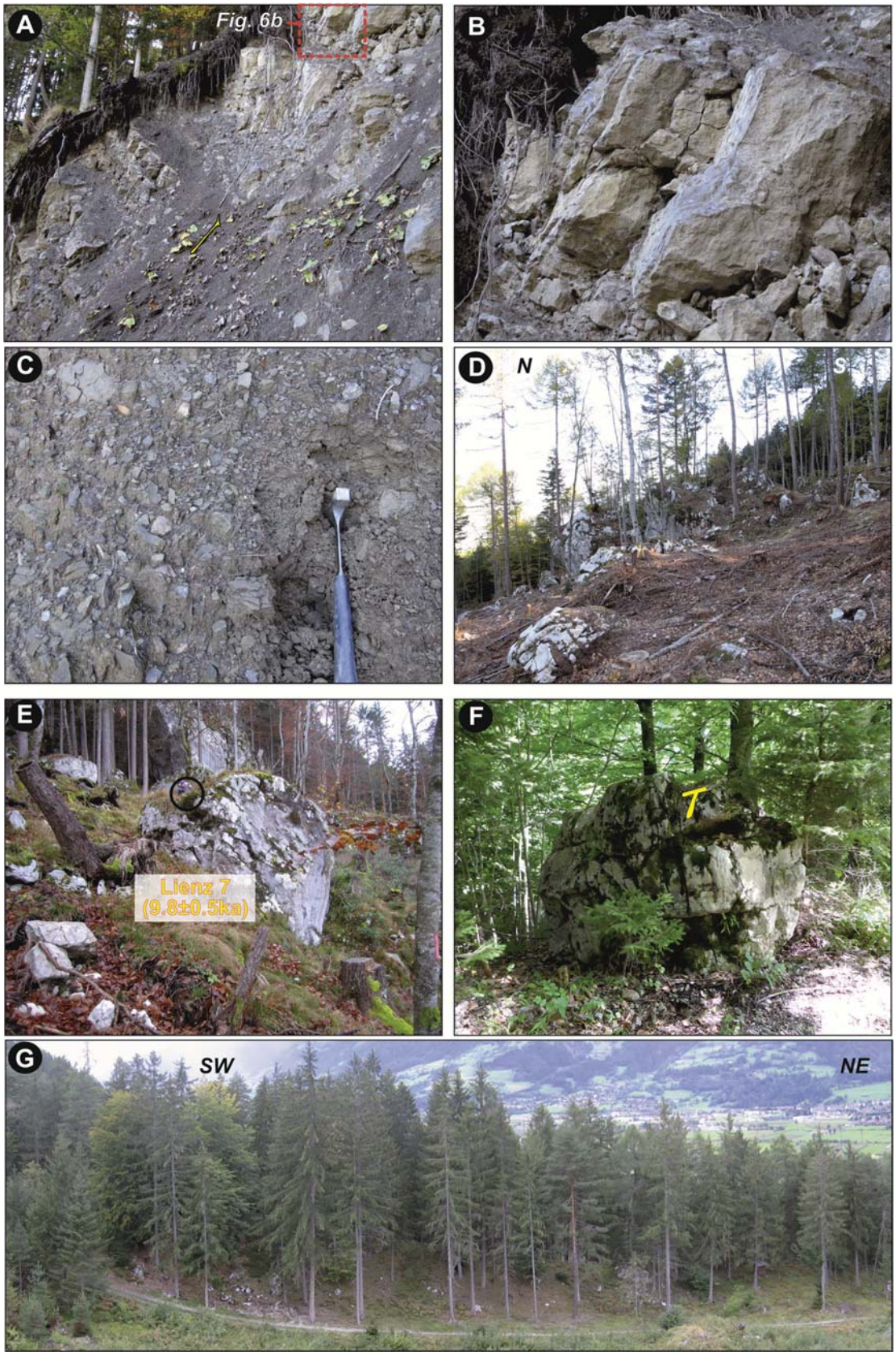
A
Fig. 6b
B
C
D
N
S
E
Lienz 7
(9.8±0.5ka)
F
T
G
SW
NE

Boulders like the one of the sample sites Lienz 5 (Fig. 4e) and Lienz 6 (Fig. 1) with a volume of up to 50 m^3 can be classified as subangular to subrounded on the surface. In contrast, rare outcrops, like A-1, exhibit just 0.5 m below the surface a clast-supported scree without matrix (SCc) consisting of very angular to angular clasts of gravel to boulder size (Fig. 4f). The surface of the clasts is coated by a ≤1 mm thick very bright, floury, calcareous precipitation. This observation indicates that the less angular clast boulder shapes on the surface are the result of weathering.

Outcrops in the deeper part (e.g. A-2) show material of the Kössen Fm. where the limestone strata are characterised by irregular fractures not in accordance with the joint patterns of the original bedrock (Fig. 4g). The amount of fragmentation changes without a sharp boundary from relatively compact limestone outcrops with an extent of some metres to very angular clasts of decimetre-size. Thus, this facies shows the characteristics of the "jigsaw-fractured (sub-)facies" described by Dufresne et al. (2016a) as part of the body facies. At the same outcrop A-2, a matrix-supported, brownish diamicton with very angular clasts in a silty-sandy matrix displays a more intensive comminution of the "fragmented (sub-)facies" (Fig. 4h). Again, very angular clasts are fragmented.

Deposition area B (Kreithof)

The middle part of the deposition area is characterised by a change of slope from around 15° above 1100 m a.s.l. to 20-25° between 1100 and 900 m a.s.l. This step occurs in the western prolongation of the bedrock ridge north of Kreithof consisting predominantly of Oberrhätkalk (Figs. 4, 5). Due to faulting (Fig. 3), this massive white limestone disappears towards the west. However, the occurrence of Hauptdolomit seems to be responsible for the increase in steepness.

The facies of the outcrops (B-1, B-2; Figs. 1, 4) is comparable to that of A-2. Large outcrops of Kössen Fm. (marly limestone to claystone; B-1 in Fig. 6a) show the lithological succession of the release area. However, the dip of the strata differs considerably from the scarp area with e.g. 315/45 to 350/52 for B-1 and 220/65 for B-2. Again, mechanically competent limestone components show an internal fragmentation with irregular fractures (B-1 in Fig. 6b). The occurrence of the fragmented subfacies (Fig. 6c) is very restricted.

In contrast, the small B-3 outcrop shows a very dense and consolidated matrix-supported diamicton (Dmm) with a greyish-green to reddish silty-clayey matrix. Based on the lithological characteristics this melange-like deposit represents most likely strongly fragmented Allgäu Fm. maybe in contact with Rotkalk marls.

The morphology of the deposition area shows in the central parts S-N-oriented longitudinal ridges with a height of less than 5 m, indicating the flow direction of the rock avalanche (Figs. 1, 5). At the eastern limit near Kreithof, a fan shaped landform with small channel-like features is evident on the DEM (Fig. 5). Drainage trenches at site B-4 show a maximum 0.5 m thick layer of a clast-rich diamicton with gravel to cobble size clasts overlying strongly commuted dark claystone of the Kössen Fm., which due to weathering, appears to be a plastic silty clay. Hence, this fan-shaped area has been mapped as a rock avalanche area which was finally shaped by a precursor of the Kohlstatt creek after the rock avalanche event.

Deposition area C (Buchwiese) with megaboulder cluster

NW of the Oberrhätkalk bedrock ridge at Kreithof, the deposition area is characterised by a cluster of outstandingly large boulders (Figs. 6d, 6e) consisting of white limestone (Fig. 5). The areal distribution of these megaboulders with a volume between 10 and c. 1000 m^3 is best described as a narrow fan with an apex on the southern end near Kreithof. No ridge-like structures are evident in this area.

The only ridge (max. height 5 m, c. 200 m length) with large but in general smaller boulders of the same lithology in this area is just outside the megaboulder cluster (C4 in Figs. 5, 6g). Rare outcrops like C-3 along the creek at the northwestern rim show that the rock avalanche deposit is underlain by polymictic delta deposits with subanglular to rounded crystalline and limestone clasts, typical for deposits of the phase of ice-decay (Reitner et al., 2016). The rock avalanche deposits in the distal part (C-2) comprise diamictons with angular Allgäu Fm. clasts in a silty-sandy matrix. In the northeastern part a small cluster of 1-2 m^3 of subangular to subrounded Rotkalk boulders (Fig. 6f) can be mapped (C-5 in Figs. 1, 5). Outcrops close to the limit of the rock avalanche deposit show a < 2 m thick deposit consisting of a matrix-supported diamicton with a silty-sandy matrix on top of mica schists. The clasts consist of lithologies of "Rotkalk" and Allgäu Fm, both originally occurring at the northern (distal) part of the scarp area.

The most distal parts of the rock avalanche deposits reach down to the alluvial deposits of the River Drau. However, no indications of such deposits further to the north, or of fluvially reworked deposits, have been found so far in this area which is nowadays intensively used for agriculture and a golf resort.

4.2. Geophysics

Profile P1 (Fig. 7a) shows a contrast between the bedrock, in this case made of mica schists with an electrical resistivity of > 900 Ωm and the rock avalanche

<<<<< ---------- ----------

Fig. 6 - Images from the field in middle (B) and lower part (C) of the deposition area. 6a) Outcrop B1 showing a fragmented alternation of limestone and claystone beds of the Kössen Fm. (dip 350/52; 0.6 m long yellow pick for scale) 6b) detail from 6a with a limestone in jigsaw facies. 6c) outcrop B1 with the rare occurrence of the fragmented facies (matrix-supported diamicton with very angular clasts) (hammer length 28 cm).6d) the megaboulder cluster at site C-1. 6e) sample site Lienz 7 within the megaboulder cluster. Encircled head of a person for scale. Note the giant boulder in the background (red X). 6f) The typical maximum size of the Rotkalk (red limestone) at site C-5 (yellow hammer for scale) Note the subangular shape. 6g) Longitudinal ridge at site C-4. Direction of view towards NW.

deposit. The latter with a thickness of up to 40 m reveals in general a low resistivity of 50-320 Ωm. Only the uppermost 10 metres can display resistivities of 900 Ωm and higher, especially in the first c. 200 m where the profile crosses the mega-boulder cluster (Fig. 5). At the SE end of the profile the bedrock crops out in accordance with the mapping results (Fig. 1).The profile P2 (Fig. 7b) reveals a less pronounced contrast between bedrock made of Lavant Fm. (siliciclactic limestone, marl, siltstone; resistivity 85-200 Ωm) and the rock avalanche deposit (30-80 Ωm). The interpreted thickness of the latter shows a strong variance of 5 to 30 m. Profile P3 (Fig. 7c) displays rock avalanche material with a maximal thickness of 10 m on top of two different bedrock lithologies (Lavant Fm. and Allgäu Fm.). Like at P1, an uppermost high resistivity layer (200-550 Ωm) occurs between profile metres 75 and 100 covering thicker rock avalanches deposits with (50-70 Ωm).

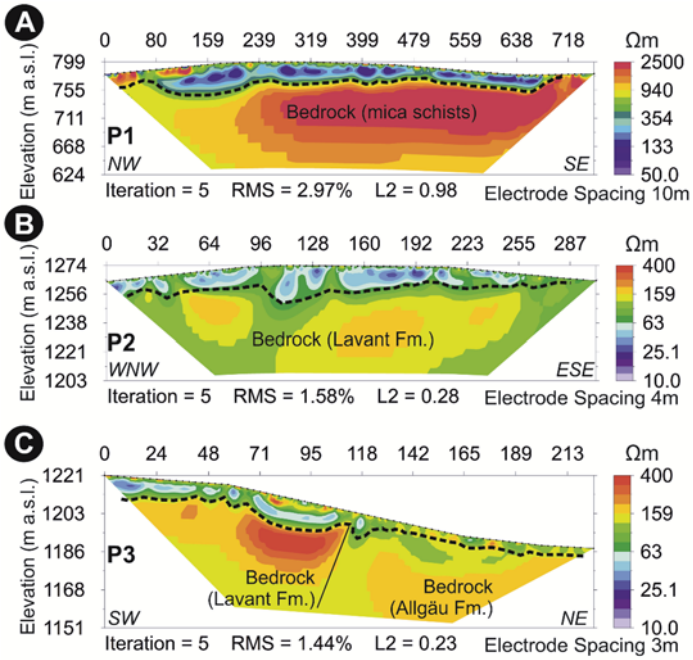

Fig. 7 - The results of the geoelectrical survey at profile P1, P2 and P3 (for location see Figs. 1, 5). Note the colour bar for restivity of P1 is different from P2 and P3.

4.3 Area, volume and Fahrböschung

The mapped rock avalanche deposits cover an area of 2.7 km^2. When considering the already eroded parts, an original area of c. 2.8 km^2 seems to be reasonable, which is four times larger than the scarp area. The results of geological mapping and geoelectrical surveying (Fig. 7) show varying rock avalanche deposit thicknesses of 2-60 m, respectively 5-40 m, and indicate that a precise estimate of the volume of the deposit is challenging. The most reliable approach is the estimate of volume based on the missing volume in the detachment niche. The scenario with a planar surface (Fig. 8a) reveals 20x10^6 m^3 whereas the more realistic one with a slightly convex surface (Fig. 8b) results in 27x10^6 m^3. This would correspond to an average 10 m thick rock avalanche deposit. However, an increase in volume of the deposit compared to the detached carbonate bedrock of 25-30% (Abele, 1974; Hungr & Evans, 2004) due to the comminution process has to be considered, resulting in a calculated average thickness of c. 13 m. Taking into account the modification of the scarp area due to small mass movements after the event, the most reliable estimate for the original maximum scarp altitude is c. 1850 m a.s.l. With the lowermost parts of the deposit at 650 m a.s.l., we have a drop height (H) of 1200 m. In combination with the runout length of the rock avalanche (L) of 3.5 km, the Buchwiese rock avalanche has a Fahrböschung α (after Heim, 1932) of 19° and a H/L ratio of 0.36. In comparison, the average slope angle of the pathway is 16°.

4.4. Age

The results of the surface exposure dating with ^{36}Cl are shown in Tab. 1. Ages range from 9.8±0.5 ka (Lienz 7) to 11.9±0.5 (Lienz 5) (Figs. 1, 5c, 6b). All four ages overlap within the given uncertainties. There is no spatial pattern with respect to the ages. The spread in ages may be attributable to processes that lead to too old ages, like inheritance, and too young ages, such as post-depositional movement of the boulder or spalling of the surface. As there is no independent means to establish which ages are the true ages, we take an average of all four ages. The average age is 10.8±0.9 ka. The uncertainty on the mean reflects both the uncertainty on the individual ages and the spread in the ages.

5. DISCUSSION

The legacy of the reconstructed Buchwiese rock avalanche with an age of 10.8±0.9 ka reveals numerous morphological and sedimentary features that indicate control by both the lithological distribution in the scarp area and the pathway morphology and geology.

5.1 Geometry

When comparing the geometry of the detachment area with that of the deposition area the fourfold areal extension (0.7 km^2 *vs.* ~2.8 km^2) of the latter is evident. This is overwhelmingly the result of an extension in the longitudinal (runout) direction (0.9 m vs. c. 3 km) and not that of a widening (0.8 km vs 1.2 km). In general, such a geometry of the rock avalanche displays the morphological conditions along the pathway with a slope allowing unconfined flow and the absence of a major obstacle with the exception of the bedrock ridge at Kreithof in the middle part (Figs. 1, 3).

The Early Holocene age provides a reasonable explanation of the sharp limit between the most distal part of the rock avalanche and the alluvial deposits of the River Drau. Considering the reconstructed progradation phases of an alluvial fan just 4 km down-valley (Patzelt & Poscher, 1995), the modern valley floor of the River Drau seems to have been in an aggradational phase since the Younger Dryas (12.8-11.7 ka) with only lateral erosion of the originally meandering River Drau (Burschil et al.,

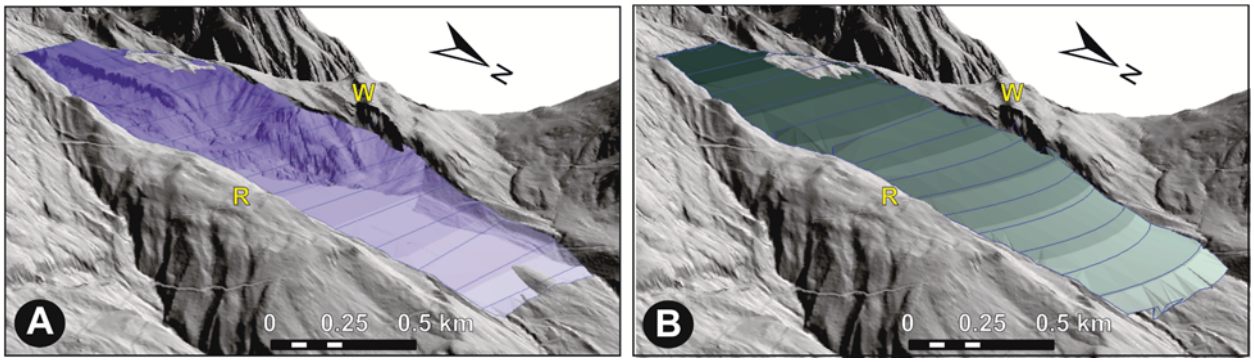

Fig. 8 - Reconstructed paleo-topographies of the scarp area for volume calculations of the detached mass. A) The scenario with a planar surface reveals $20x10^6$ m^3 B) The scenario with a slightly convex surface results in $27x10^6$ m^3.

2019). Thus, any remnants of the rock avalanche north of the current limit, if they ever existed, must have been reworked. The presence of a thick layer of Buchwiese rock avalanche deposits in the centre of the valley can be ruled out (Burschil et al., 2019).

A limited amount of uncertainty exists regarding the extension in two cases. The fan-like structure of the partly reworked deposit south of Kreithof could potentially indicate a branch towards the east. However, no further traces of the rock avalanche have been found in the catchment of the eastward draining creek. The other case concerns the relation between the rock avalanche deposit on the northwestern limits and the Lake Tristach basin. The latter is the result of subglacial shaping. Alluvial fans nowadays constrain the eastern limit of the lake. However, a further extension of this small basin and maybe the lake towards the east, in the range of few hundred metres, into the area now covered by the alluvial fans and parts of the rock avalanche seems to be likely. Thus, a subordinate branch of the Buchwiese rock avalanche flowing towards the west into the area now covered by the modern Lake Tristach cannot be ruled out without limnogeological investigations.

5.2. Morphology, lithological distribution and facies

Ridges within the rock avalanche deposit are the most evident morphological indicators of fluid-like runout motion. All mapped features in the study area are best interpreted as longitudinal ridges (Dufresne & Davies, 2008). The most prominent one in terms of length and height occurs in deposition area A with the Lienz 5 boulder on top (Fig. 1). According to the lithology of the boulders (massive limestone from Oberrhätkalk) its formation started already after around 600 m. The same lithology is evident at ridge at C-4 in the lowermost deposition area C. Smaller ridges consist of Kössen limestone. Considering the topographic conditions enabling unhindered spreading, the presence of ridges in the case of the Buchwiese rock avalanche seems to be linked to the availability of sufficient mechanically competent material (Dufresne & Davies, 2009) such as limestone. In contrast, the less competent materials of the Kössen Fm. (marl, claystone) were not able to form such ridges.

This lithological control is also evident in the facies of the deposits. The occurrence of a blocky, clast-supported carapace facies overlying a body facies (Dunning, 2004; Weidinger et al., 2014; Dufresne et al., 2016a) is a common feature in rock avalanche deposits (e.g. Dufresne et al., 2016b; Reitner et al., 2018; Singeisen et al., 2020). Such a carapace facies is only present at the ridges and in other limited areas where limestone especially the massive Oberrhätkalk occurs, e.g. in the megaboulder cluster. Despite the absence of large outcrops, which would allow tracing the changes of facies and fragmentation with depth, the available outcrop and geoelectrical data show in general the typical succession of a rock avalanche: Below a carapace facies, if present, clast-supported diamictons (A-1 in Fig. 4e) occur which resemble the blocky facies of Dufresne et al. (2016a). Outcrops of the interior in the deposition areas A and B consist mostly of strongly fragmented rock (outcrops A-2 and B-1 in Figs. 4e, g, h) which represent the jigsaw subfacies of Dufresne et al (2016a). In comparison, the occurrence of matrix-supported diamicton, the fragmented subfacies appears to be limited (e.g. lower part of outcrop A-2; Fig. 4f). The rare outcrops of the deeper part of deposition area C only show the fragmented subfacies.

Geophysical data (in Fig.7) also display the different amounts of fragmentation. The carapace facies in P1 (megaboulder cluster) and P3 is easy to identify. However, an absolute quantification of the degree of fragmentation via the resistivity values (in Ωm) seems to be problematic due to the lithological variations of the fragmented source rocks within the profiles.

The megaboulder cluster represents within the distal deposition area C, an outstanding and rather isolated feature. It is the largest coherent area with carapace facies comprising some Oberrhätkalk limestone boulders of enormous size of up to 1000 m^3. The fan-shaped distribution with an apex just below the western edge of the Kreithof Oberrhätkalk bedrock ridge provides a clue for the provenance of the megaboulders. According to the most likely scenario, the western part of the glacially shaped bedrock ridge was impacted and eventually detached by the rock avalanche. The fan-like distribution and limited fragmentation as shown by the carapace facies support this suspected style of formation.

Excluding the megaboulder cluster, the distribution of lithologies within the rock avalanche deposit mirrors the sedimentary succession in the detachment area, with the clasts of the Rotkalk and Allgäu Fm. in the most

distal part. As in other cases (Heim, 1932; Strom, 2006; Hewitt et al., 2008; Dufresne et al., 2016a, b; Rossato et al., 2020a), the preserved source stratigraphy within the dilated rock mass is a clear argument for a predominantly laminar style of rock avalanche movement.

5.3 The age, chronology of failure, kinematics, and its implications

The age of the Buchwiese rock avalanche of 10.8±0.9 ka, based on averaging of all four boulder ages, is in accordance with the superposition of the deposit on top of Lateglacial delta deposits (phase of ice-decay, Reitner et al., 2016) and the evident rounding of the boulders due to carbonate dissolution since deposition. The age also shows that the rock slope failure occurred 8-9 ka after the last glacial shaping and oversteepening of the slope during the LGM.

The weakest lithology in the source area are the marls and claystones, i.e. the slaking rocks of the Kössen Fm. Fatigue of this material over some thousand years together with the general dip-slope situation are regarded as the main cause for the slope failure and the detachment of a rock mass as a translational slide (Cruden & Varnes, 1996) or rock planar slide (Hungr et al., 2014). NNE-SSW trending faults facilitated the formation of the niche which finally developed with a mostly plane sliding surface (Fig. 3), which also cut through the competent Oberrhätkalk as well as the Allgäu Fm. Tension gaps, which are still present in the stable margin, most likely were the precursors of the slope failure. In such a setting with alternations of fine-grained aquicludes and fractured aquifer within brittle limestone (Probst et al., 2003), variations in the hydrostatic pressure over time were likely an additional driver for the slope failure.

Currently there is no indication of a trigger like a paleo-earthquake documented in other archives nearby. In addition, the regional seismicity is low (Reiter et al., 2018). The slope failure occurred during the Preboreal, a stage known for a considerable warming trend and its dryness (Schmidt et al., 2006; Magny et al., 2007; Ilyashuk et al., 2011), which makes in general a higher wetness associated with high hydrostatic pressure in the jointed rocks as a cause / trigger unlikely. Nevertheless, Magny (2004) reported evidence of a distinctly wetter phase with higher lake-levels in Central Europe at 10.3-10.0 ka, which does overlap with the Buchwiese failure event within the given error range. When comparing the altitude of the source area with the known spatial development in the region (Steinemann et al., 2020), permafrost could have occurred for the last time during the Younger Dryas. Permafrost degradation associated with the marked warming around 10.5 ka (Ivy-Ochs et al., 2009; Protin et al., 2019) may have contributed to the weakening of the slope (Krautblatter et al., 2013) as well.

In such a geological setting, the detachment occurred in the initial phase as a translational slide. The onset of the first ridge after a travel distance of approx. 600 m shows a nearly instantaneous fragmentation leading to the typical fluid-like behaviour of a rock avalanche. Such a strong fragmentation is especially evident in the brittle limestone. In comparison, large outcrops of Kössen Fm. debris upstream of the Kreithof ridge with a comparable moderate fragmentation in the middle part of the flow, may indicate a longer sliding phase within this lithology due to the preferential deformation of the weak claystone layers. The pathway shows a slight bending NNE to NE at the south-eastern flank of the Rauchkofel peak. Such a flowline could have been predetermined to some extent by pre-existing paleo-valleys. After this, the strongest interference with topography occurred by the collision with at least parts of the western limestone ridge extension at Kreithof (Fig. 5). On the one hand, this development led to the formation of the megaboulder cluster. Due to the break in slope a jump of less than 200 m could have occurred. On the other hand, the rock avalanche smoothed the glacially shaped topography south of the glacially moulded bedrock ridge which explains the greatest thickness in this area (Fig. 3).

After the assumed short-distance jump, the rock-avalanche moved with more or less the same width leading to further fragmentation. The patchy coverage in the areas close to the alluvial deposits of the River Drau together with a thinning of the rock avalanche cover indicate the final run-out. The facies and the morphology of the deposits are in accordance with the hypotheses of dynamic fragmentation (McSaveney & Davies, 2006; Davies & McSaveney, 2009) as the main mechanical reason for reducing the internal friction of the moving mass and, eventually, the long run-out.

5.4 Comparison with other catastrophic slope failures

The Buchwiese is one of the rare cases of an unconfined rock avalanche which remained on the slope and did not reach the valley floor. Most of the rock avalanches discussed in recent years are characterised either by events which hit the valley floor or had interactions with valley flanks (e.g. Hewitt et al., 2008; Ostermann et al., 2012; Grämiger et al., 2016; Ivy-Ochs et al., 2017). Hence comparison with respect to the kinematics and the influence of topographic obstacles and constraints is not an easy task.

Based on available data under dip-slope conditions, the Kössen Fm. tends to fail as slides or relatively slow flows or a combination of these (Nickmann, 2009; Nickmann & Thuro, 2013; Lotter & Gruber, 2020). In cases with a dip much steeper than the slope, catastrophic rock slides are known, like the two cases (Mordbichl, Lienzer Klause) from the northwestern flank of Lienz Dolomites in the upper Drau Valley (Puster Valley; Reitner, 2003a, 2016; Linner et al., 2013). Such a tectonic setting, different from the Buchwiese scarp area, may explain the formation of a listric sliding plane, independent of the bedding in the cases of Puster Valley.

In general, the Lienz Dolomites, despite their high relief, do not have an abundance of catastrophic rock slope failures. Beside the Buchwiese and the two rockslides (Mordbichl, Lienzer Klause) with a Late Holocene age, only the Laserz rock avalanche consisting of fragmented dolostone occurred during a Younger Dryas glacier advance (Reitner et al., 2014). Within a distance of 25 km there are only two additional cases within crys-

talline tectonic units, Feld near Matrei (Reuther et al., 2006) and Kals (Veit, 1988), which are altogether not linked to one tectonic system as has been noted at other sites (Brenner cluster - Ostermann & Sanders, 2017; Piave Valley - Rossato et al., 2020b).

There has been some discussion of a temporal cluster of large landslides in the Alps during the Early Holocene, which comprised the Kandersteg, Flims and Koefels events (Ivy-Ochs et al., 2017 and references therein). Indeed, the recently presented ^{36}Cl exposure age, 3.2±0.2 ka, for the Kandersteg event (1.1 km^3) weaken this conjecture as the Kandersteg event occurred during the Late and not the Early Holocene (Singeisen et al., 2020). By comparing the Buchwiese age of 10.8±0.9 ka with other dated events in the Alps it is evident that dated Early Holocene catastrophic rock slope failure are rare when comparing with the available records (Prager et al., 2008; Ivy-Ochs et al., 2017). The two largest events in the Alps, Flims (10-12 km^3) and Köfels (3 km^3) with ages of 9.4 ka (von Poschinger & Haas, 1997) and 9.5 ka (Nicolussi et al., 2015), overlap with the Buchwiese event within the age uncertainties. Nevertheless, the fact that the sites are distant from each other makes implicating a seismic trigger difficult. The strongest age overlap is with the rather small Lenzanger rock avalanche (10.8±1.1 ka) in the Hohen Tauern mountain range. Those deposits overlie both a Younger Dryas till and the Durchgangwald rockslide deposits (12.6±1.0 ka; Bichler et al., 2016). The marked warming around 10.5 ka in the Alps, expressed as retreat of glaciers back to as small as or smaller than their Little Ice Age extents (Schimmelpfennig et al., 2012; Protin et al., 2019) and especially as permafrost degradation, may have been the critical factor that led to slope failure at Buchwiese. Nevertheless, the release area itself is not in an area occupied by a glacier during the Younger Dryas (Reitner et al., 2016).

6. CONCLUSIONS

We present reconstruction of the Buchwiese rock avalanche based on geological field mapping, analysis of DEM data, ^{36}Cl exposure dating, and a geoelectrical survey. Based on the results of the ^{36}Cl exposure dating, the event took place at 10.8±0.9 ka during the Early Holocene and, thus, 8-9 ka after the last glacial shaping and oversteepening of the slope during the LGM. The age is the average of all four obtained boulder ages.

The failure of a rock mass with a volume of 27x10^6 m^3 was enabled by dip-slope sliding within strata of the Kössen Fm. (limestone, marls, claystone), Oberrhätkalk (massive to thickly bedded limestone), and Rotkalk (red nodular limestone and marl) dipping to the north in combination with N-S to NNE-SSW running brittle faults. Weak layers in the fine-grained rocks of the Kössen Fm. (claystone, marl) are the major lithological precondition for the mass movement. We consider fatigue of such slaking rocks since the LGM as the major cause for this catastrophic rock slope failure.

According to the geological conditions, the initial failure occurred as a translational slide with a mostly plane sliding surface. In the deposition area, strong control of lithology and topography on the development of different facies and morphological features is evident:

1. Longitudinal ridges indicate spreading of an unconfined flow. The onset of the first longitudinal ridges shows a strong fragmentation resulting in fluid-like movement after only 600 m of transport. The most prominent ridges with respect to height and length consist of the massive Oberrhätkalk. Smaller ridges are developed in Kössen limestone whereas the other lithologies were not able to form ridges.
2. The carapace facies consisting of clast-supported boulders is only developed in areas with limestone (mostly Oberrhätkalk but also limestone of the Kössen Fm.).
3. The body facies in the upper parts (deposition area A) are dominated by the jigsaw subfacies with a subordinate occurrence of fragmented subfacies in the outcrops. Even in the middle part (area B) the prevalence of the moderately fragmented jigsaw subfacies within large soutcrops of Kössen Fm. consisting of alternating claystone, limestone beds is evident. This may indicate preferential deformation within the claystone beds.
4. After partial collision with a bedrock ridge consisting of massive Oberrhätkalk limestone and a small jump, the fragmented facies dominates.
5. This collision led to the formation of megaboulder cluster consisting of detached and fragmented Oberrhätkalk boulders with volumes of up to 1000 m^3 and a fan-like distribution.

The preserved source stratigraphy within the dilated rock mass is a clear argument for a predominantly laminar style of rock avalanche movement. This finding, together with the presence of longitudinal ridges indicating fluidisation, as well as the facies distribution, support the dynamic fragmentation model (McSaveney & Davies, 2006; Davies & McSaveney, 2009) as the best mechanical explanation for the Buchwiese rock avalanche.

ACKNOWLEDGEMENTS

Comments provided by Jeff Moore and an anonymous reviewer helped us to improve the paper. We are grateful for the help of Hanns Kerschner during sampling in November 2007. Discussions with Bernd Imre in 2011 in the field and with Michael Lotter and Marc Ostermann at the Geological Survey of Austria were helpful in refining the interpretation of fragmentation and mechanics. Ruth Drescher-Schneider provided valuable information on the paleoclimatic conditions. We would also like to thank Stefanie Gruber, Stefan Pfeiler, Ivo Baron and Anna Zöchbauer for support at the geophysical survey, and the accelerator mass spectrometry group at Ion Beam Physics ETH Zurich and especially to Vasily Alfimov for AMS ^{36}Cl measurements.

REFERENCES

Aaron J., McDougall S. (2019) - Rock avalanche mobility: The role of path material. Engineering Geology, 257, 105126.

Aaron J., Wolter A., Loew S., Volken S. (2020) - Understanding Failure and Runout Mechanisms of the

Flims Rockslide/Rock Avalanche. Frontiers in Earth Science, 8, 224, 1-19.
Abele G. (1974) - Bergstürze in den Alpen, ihre Verbreitung, Morphologie und Folgeerscheinungen. Wissenschaftliche Alpenvereinshefte, 25, 230.
Alfimov V., Ivy-Ochs S. (2009) - How well do we understand production of 36Cl in limestone and dolomite?. Quaternary Geochronology, 4(6), 462-474.
Aizebeokhai A.P. (2010) - 2D and 3D geoelectrical resistivity imaging: Theory and field design, Scientific Research and Essay, 5(23), 3592-3605.
André M.F. (2002) - Rates of postglacial rock weathering on glacially scoured outcrops (Abisko-Riksgränsen area, 68° N). Geografiska Annaler: Series A, Physical Geography, 84(3-4), 139-150.
Bauer W. (1990) - Geologische Kartierung in den nordöstlichen Lienzer Dolomiten (Tirol). Master Thesis (Diplomarbeit), Rheinland Westfälische Technische Hochschule Aachen.
Bichler M.G., Reindl M., Reitner J.M., Drescher-Schneider R., Wirsig C., Christl M., Hajdas I., Ivy-Ochs S. (2016) - Landslide deposits as stratigraphical markers for a sequence-based glacial stratigraphy: a case study of a Younger Dryas system in the Eastern Alps. Boreas, 45, 537-551.
Blau J., Grün B. (1995) - Jura und Kreide in der Amlacher Wiesen-Mulde (Nördliche Lienzer Dolomiten). Arbeitstagung der Geologischen Bundesanstalt. Geologie von Osttirol, Lienz, 43-66, Geologische Bundesanstalt, Vienna.
Brandner R., Gruber A., Prager C., Lutz D., Ortner H. (2001) - Regional extension between meso-alpine and neo-Alpine compressional structural systems north and south of the Periadriatic lineament (Lienz Dolomites and eastern Southern Alps). Geologisch-Paläontologische Mitteilungen. Innsbruck, 25, 52-54.
Burschil T., Tanner D.C., Reitner J.M., Buness H., Gabriel G. (2019) - Unravelling the shape and stratigraphy of a glacially-overdeepened valley with reflection seismic: The Lienz Basin (Austria). Swiss Journal of Geosciences, 112(2-3), 341-355.
Christl M., Vockenhuber C., Kubik P.W., Wacker L., Lachner J., Alfimov V., Synal H.A. (2013) - The ETH Zurich AMS facilities: Performance parameters and reference materials. Nuclear Instruments and Methods in Physics Research Section B: Beam Interactions with Materials and Atoms, 294, 29-38.
Crosta G.B., Frattini P., Fusi N. (2007) - Fragmentation in the Val Pola rock avalanche, Italian alps. Journal of Geophysical Research: Earth Surface, 112(F1).
Cruden D.M., Varnes D.J. (1996) - Landslides: investigation and mitigation. Chapter 3-Landslide types and processes. Transportation research board special report, 247, 36-75.
Dahlin T., Bing Z. (2006) - Multiple-gradient array measurements for multichannel 2D resistivity imaging, Near Surface Geophysics, 4(2), 113-123.
Davies T.R., McSaveney M.J. (2009) - The role of rock fragmentation in the motion of large landslides. Engineering Geology, 109(1), 67-79.
Dufresne A., Davies T.R. (2009) - Longitudinal ridges in mass movement deposits. Geomorphology, 105(3-4), 171-181.
Dufresne A., Bösmeier A., Prager C. (2016a) - Sedimentology of rock avalanche deposits-case study and review. Earth-Science Reviews, 163, 234-259.
Dufresne A., Prager C., Bösmeier A. (2016b) - Insights into rock avalanche emplacement processes from detailed morpho-lithological studies of the Tschirgant deposit (Tyrol, Austria). Earth Surface Processes and Landforms, 41(5), 587-602.
Dufresne A., Dunning S.A. (2017) - Process dependence of grain size distributions in rock avalanche deposits. Landslides, 14(5), 1555-1563.
Dunning S.A. (2004) - Rock avalanches in high mountains-A sedimentological approach. Unpublished PhD Thesis University of Luton, UK.
Eisbacher G.H., Clague J.J. (1984) - Destructive mass movements in high mountains: hazard and management, Geological Survey of Canada, Vancouver, British Columbia, Canada.
Erismann T.H., Abele G. (2001) - Dynamics of rockslides and rockfalls. Springer-Verlag Berlin Heidelberg, Germany.
Grämiger L.M., Moore J.R., Vockenhuber C., Aaron J., Hajdas I., Ivy-Ochs S. (2016) - Two early Holocene rock avalanches in the Bernese alps (Rinderhorn, Switzerland). Geomorphology, 268, 207-221.
Heim A. (1932) - Bergsturz und Menschenleben, Vierteljahrsschrift der Naturforschenden Gesellschaft in Zürich, 20, Beer & Co., Zürich.
Hewitt K., Clague J.J., Orwin J.F. (2008) - Legacies of catastrophic rock slope failures in mountain landscapes. Earth-Science Reviews, 87(1-2), 1-38.
Hungr O., Evans S.G. (2004) - Entrainment of debris in rock avalanches: an analysis of a long run-out mechanism. Geological Society of America Bulletin, 116(9-10), 1240-1252.
Hungr O., Corominas J., Eberhardt E. (2005) - Estimating landslide motion mechanism, travel distance and velocity. In Landslide risk management (pp. 109-138). CRC Press.
Hungr O., Leroueil S., Picarelli L. (2014) - The Varnes classification of landslide types, an update. Landslides, 11(2), 167-194.
Ilyashuk E.A., Koinig K.A., Heiri O., Ilyashuk B.P., Psenner R. (2011) - Holocene temperature variations at a high-altitude site in the Eastern Alps: a chironomid record from Schwarzsee ob Sölden, Austria. Quaternary Science Reviews, 30(1-2), 176-191.
Imre B., Laue J., Springman S.M. (2010) - Fractal fragmentation of rocks within sturzstroms: insight derived from physical experiments within the ETH geotechnical drum centrifuge. Granular matter, 12 (3), 267-285.
Ivy-Ochs S., Synal H. A., Roth C., Schaller M. (2004) - Initial results from isotope dilution for Cl and ^{36}Cl measurements at the PSI/ETH Zurich AMS facility. Nuclear Instruments and Methods in Physics Research Section B: Beam Interactions with Materials and Atoms, 223, 623-627.
Ivy-Ochs S., Kober F. (2008) - Surface exposure dating with cosmogenic nuclides. E&G Quaternary Science Journal, 57(1-2), 179-209.
Ivy-Ochs S., Kerschner H., Maisch M., Christl M., Kubik

P.W., Schlüchter C. (2009) - Latest Pleistocene and Holocene glacier variations in the European Alps. Quaternary Science Reviews, 28(21), 2137-2149.

Ivy-Ochs S. (2015) - Glacier variations in the European Alps at the end of the last glaciation. Cuadernos de investigación geográfica/Geographical Research Letters, 41(2), 295-315.

Ivy-Ochs S., Martin S., Campedel P., Hippe K., Alfimov V., Vockenhuber C., Andreotti E., Carugati G., Pasqual D., Rigo M,. Viganò A. (2017) - Geomorphology and age of the Marocche di Dro rock avalanches (Trentino, Italy). Quaternary Science Reviews, 169, 188-205.

Keller B. (1996) - Lithofazies-Codes für die Klassifikation von Lockergesteinen. Mitteilungen der Schweizerischen Gesellschaft für Boden- und Felsmechanik, 132, 5-12.

Krautblatter M., Funk D., Günzel F.K. (2013) - Why permafrost rocks become unstable: a rock-ice-mechanical model in time and space. Earth Surface Processes and Landforms, 38(8), 876-887.

Linner M., Reitner J.M., Pavlik W. (2013) - Geologische Karte der Republik Österreich 1:50.000 Blatt 179 Lienz. Geologische Bundesanstalt, Vienna.

Loke M.H. (2019) - Geoelectrical Imaging 2-D & 3-D, Manual, Geotomo Software, Malaysia.

Loke M.H., Chambers J.E., Rucker D.F., Kuras O., Wilkinson P.B. (2013) - Recent developments in the direct-current geoelectrical imaging method, Journal of Applied Geophysics, 95, 135-156.

Lotter M., Gruber A. (2020) - Ingenieurgeologie - Geogene Naturgefahren. - In: Gruber A., Lotter M., Brandner R. (eds.): Erläuterungen zur Geologischen Karte der Republik Österreich 1:50.000, Blatt 88 Achenkirch, 200-230, Geologische Bundesanstalt, Vienna.

Magny M. (2004) - Holocene climate variability as reflected by mid-European lake-level fluctuations and its probable impact on prehistoric human settlements. Quaternary International, 113(1), 65-79.

Magny M., Vannière B., de Beaulieu J.L., Bégeot C., Heiri O., Millet L., Peyron O., Walter-Simonnet A.V. (2007) - Early-Holocene climatic oscillations recorded by lake-level fluctuations in west-central Europe and in central Italy. Quaternary Science Reviews, 26 (15), 1951-1964.

McSaveney M.J., Davies T. (2006) - Inferences from the morphology and internal structure of rockslides and rock avalanches rapid rock mass flow with dynamic fragmentation. In: Evans G. E., Mugnozza G. S., Storm A. Hermanns R. L.(eds.): Landslides from Massive Rock Slope Failure, 285-304, Springer, Dodrecht.

Monegato G., Ravazzi C., Donegana M., Pini R., Calderoni G., Wick L. (2007) - Evidence of a two-fold glacial advance during the last glacial maximum in the Tagliamento end moraine system (eastern Alps). Quaternary Research, 68(2), 284-302.

Nickmann M. (2009) - Abgrenzung und Klassifizierung veränderlich fester Gesteine unter ingenieurgeologischen Aspekten. Münchner Geowissenschaftliche Abhandlungen, Reihe B, Band 12, Verlag Dr. Friedrich Pfeil, München.

Nickmann M., Thuro K. (2013) - Die veränderlich festen Mergelsteine der Kössen-Formation als Schlüsselhorizonte für Hangbewegungen im Spitzingseegebiet (Nördliche Kalkalpen). 19. Tagung für Ingenieurgeologie mit Forum für junge Ingenieurgeologen, München 2013, 229-234.

Nicolussi K., Spötl C., Thurner A., Reimer P.J. (2015) - Precise radiocarbon dating of the giant Köfels landslide (Eastern Alps, Austria). Geomorphology, 243, 87-91.

Ostermann M., Sanders D. (2017) - The Benner pass rock avalanche cluster suggests a close relation between long-term slope deformation (DSGSDs and translational rock slides) and catastrophic failure. Geomorphology, 289, 44-59.

Ostermann M., Sanders D., Prager C., Kramers J. (2007) - Aragonite and calcite cementation in "boulder-controlled" meteoric environments on the Fern Pass rockslide (Austria): implications for radiometric age dating of catastrophic mass movements. Facies, 53(2), 189-208.

Ostermann M., Sanders D., Ivy-Ochs S., Alfimov V., Rockenschaub M., Römer A. (2012) - Early Holocene (8.6 ka) rock avalanche deposits, Obernberg valley (Eastern Alps): Landform interpretation and kinematics of rapid mass movement, Geomorphology, 171-172, 83-93.

Ostermann M., Ivy-Ochs S., Sanders D., Prager C. (2017) - Multi-method (^{14}C, ^{36}Cl, ^{234}U/^{230}Th) age bracketing of the Tschirgant rock avalanche (Eastern Alps): implications for absolute dating of catastrophic mass-wasting. Earth Surface Processes and Landforms, 42(7), 1110-1118.

Pánek T. (2019) - Landslides and Quaternary climate changes - the state of the art. Earth-Science Reviews, 196, 102871.
Doi: 10.1016/j.earscirev.2019.05.015

Patzelt G., Poscher G. (1995) - Neue Ergebnisse zur Quartärgeologie Osttirols: Fazies und Sedimentations-geschichte des Frauenbach-Schwemmfächers bei Lavant. Arbeitstagung der Geologischen Bundesanstalt. Geologie von Osttirol, Lienz, 67-73, Geologische Bundesanstalt, Vienna.

Perrone A., Iannuzzi A., Lapenna V., Lorenzo P., Piscitelli S., Rizzo E. (2004) - High-resolution electrical imaging of the Varco d'Izzo earthflow (southern Italy), Journal of Applied Geophysics 56(1), 17-29.

Prager C., Zangerl C., Patzelt G., Brandner R. (2008) - Age distribution of fossil landslides in the Tyrol (Austria) and its surrounding areas. Natural Hazards and Earth System Sciences, 8(2), 377-407.

Prager C., Ivy-Ochs S., Ostermann M., Synal H.A., Patzelt G. (2009) - Geology and radiometric ^{14}C-, ^{36}Cl-and Th-/U-dating of the Fernpass rockslide (Tyrol, Austria). Geomorphology, 103(1), 93-103.

Probst G., Brandner R., Hacker P., Heiss G., Prager C. (2003) - Hyrogeologische Grundlagenstudie Westliche Gailtaler Alpen/Lienzer Dolomiten (Kärnten/ Osttirol). Steirische Beiträge zur Hydrogeologie, 54, 5-62.

Protin M., Schimmelpfennig I., Mugnier J.L., Ravanel L., Le Roy M., Deline P., Favier V., Buoncristiani J.-F.,

Aumaître G., Bourlès D.L., Keddadouche K. (2019) - Climatic reconstruction for the Younger Dryas/early Holocene transition and the Little Ice Age based on paleo-extents of Argentière glacier (French Alps). Quaternary Science Reviews, 221, 105863. Doi: 10.1016/j.quascirev.2019.105863

Reitner J.M. (2016) - Bericht 2001-2003 über geologische Aufnahmen im Quartär auf Blatt 179 Lienz und Blatt 178 Hopfgarten in Defereggen. Jahrbuch der Geologischen Bundesanstalt, 156, 289-292.

Reitner J.M. (2003a) - Bericht 2000 über geologische Aufnahmen im Quartär auf Blatt 179 Lienz. Jahrbuch der Geologischen Bundesanstalt, 143, 391-397.

Reitner J.M. (2003b) - Bericht 1998-99 über geologische Aufnahmen im Quartär und Kristallin auf Blatt 179 Lienz. Jahrbuch der Geologischen Bundesanstalt, 143, 514-522.

Reitner J.M., Linner M. (2009) - Formation and Preservation of Large Scale Toppling Related to Alpine Tectonic Structures, Eastern Alps. Austrian Journal of Earth Sciences, 102(2), 69-80.

Reitner J.M., Ivy-Ochs S., Hajdas I., Lattner D. (2014) - Bergstürze in den Lienzer Dolomiten vom Würm-Spätglazial bis in das jüngste Holozän. - In: Koinig K.A., Starnberger R., Spötl, C. (eds.): DEUQUA 2014: 37. Hauptversammlung der deutschen Quartärvereinigung Innsbruck 2014, 24-29 September, Abstractband 96, Innsbruck (Innsbruck University Press).

Reiter F., Freudenthaler C., Hausmann H., Ortner H., Lenhardt W., Brandner R. (2018) - Active seismotectonic deformation in front of the Dolomites indenter, Eastern Alps. Tectonics, 37(12), 4625-4654.

Reitner J.M., Ivy-Ochs S., Drescher-Schneider R., Hajdas I., Linner M. (2016) - Reconsidering the current stratigraphy of the Alpine Lateglacial: Implications of the sedimentary and morphological record of the Lienz area (Tyrol/Austria). E & G Quaternary Science Journal, 65(2), 113-144.

Reitner J.M., Ostermann M., Schuster R., Bichler M.G., Knoll T., Robl J., Ivy-Ochs S. (2018) - Der Bergsturz vom Auernig (Mallnitz/Kärnten), seine Altersstellung und Folgen. Carinthia II, 208(128), 503-548.

Reitner J.M., Menzies J. (2020) - Microsedimentology of tills near Ainet, Austria-were palaeo-ice streams in the European Alps underlain by soft deforming bed zones?. Austrian Journal of Earth Sciences, 113(1), 71-86.

Reuther A.U., Reitner J.M., Ivy-Ochs S., Herbst, P. (2006) - From kinematics to dating the Sturzstrom deposit of Feld (Matrei/Eastern Tyrol/Austria). Geophys. Res. Abstr. 8, 04947.

Rossato S., Ivy-Ochs S., Martin S., Viganò A., Vockenhuber C., Rigo M., Monegato G., Zorzi M.D., Surian N., Campedel P., Mozzi P. (2020a) - Timing, drivers and impacts of the historic Masiere di Vedana rock avalanche (Belluno Dolomites, NE Italy). Natural Hazards and Earth System Sciences, 20, 2157-2174.

Rossato S., Ghirotti M., Gabrieli F., Livio F., Bovo F., Brezzi L., Campedel P., Cola S., Ivy-Ochs S., Martin S., Mozzi P., Pasuto A., Rigo M., Simonini P., Surian N., Viganò A., Vockenhuber C., Wolter A. (2020b) - Learning from the past to face the future: landslides in the Piave Valley (Eastern Alps, Italy). Alpine and Mediterranean Quaternary, 33, 2, 209-228. Doi: 10.26382/AMQ.2020.14

Schmidt R., van der Bogaard C., Merkt J., Müller J. (2002) - A new Lateglacial chronostratigraphic tephra marker for the southeastern Alps: The Neapolitan Yellow Tuff (NYT) in Längsee (Austria) in the context of a regional biostratigraphy and paleoclimate. Quaternary International, 88(1), 45-56.

Schmidt R., Kamenik C., Tessadri R., Koinig K.A. (2006) - Climatic changes from 12,000 to 4,000 years ago in the Austrian Central Alps tracked by sedimentological and biological proxies of a lake sediment core. Journal of Paleolimnology, 35(3), 491-505.

Schmid S.M., Fügenschuh B., Kissling E., Schuster R. (2004) - Tectonic map and overall architecture of the Alpine orogen. Eclogae Geologicae Helvetiae, 97(1), 93-117.

Schmidt T. (1995) - Zur Tektonik der Lienzer Dolomiten. Arbeitstagung der Geologischen Bundesanstalt. Geologie von Osttirol, Lienz, 37-42, Geologische Bundesanstalt, Vienna.

Schimmelpfennig I., Schaefer J.M., Akçar N., Ivy-Ochs S., Finkel R.C., Schlüchter C. (2012) - Holocene glacier culminations in the Western Alps and their hemispheric relevance. Geology, 40(10), 891-894.

Schuster R., Daurer A., Krenmayr H.G., Linner M., Mandl G.W., Pestal G., Reitner J.M. (2014) - Rocky Austria; the geology of Austria - brief and colourful. Geologische Bundesanstalt, Vienna.

Singeisen C., Ivy-Ochs S., Wolter A., Steinemann O., Akçar N., Yesilyurt S., Vockenhuber C. (2020) - The Kandersteg rock avalanche (Switzerland): integrated analysis of a late Holocene catastrophic event. Landslides, 17, 1297-1317.

Steinemann O., Reitner J.M., Ivy-Ochs S., Christl M., Synal H.A. (2020) - Tracking rockglacier evolution in the Eastern Alps from the Lateglacial to the early Holocene. Quaternary Science Reviews, 241, 106424. Doi: 10.1016/j.quascirev.2020.106424

Strom A. (2006) - Morphology and internal structure of rockslides and rock avalanches: grounds and constraints for their modelling. In Landslides from massive rock slope failure, 305-326. Springer, Dordrecht.

van Husen D. (2000) - Geological processes during the Quaternary. Mitteilungen der Österreichischen Geologischen Gesellschaft, 92(1999), 135-156.

Veit H. (1988) - Fluviale und solifluidale Morphodynamik des Spät- und Postglazials in einem zentralalpinen Flusseinzugsgebiet (südliche Hohe Tauern, Osttirol). - Bayreuther Geowissenschaftliche Arbeiten, 13, 1-167.

Vockenhuber C., Miltenberger K.U., Synal H.A. (2019) - ^{36}Cl measurements with a gas-filled magnet at 6 MV. Nuclear Instruments and Methods in Physics Research Section B: Beam Interactions with Materials and Atoms, 455, 190-194.

von Poschinger A., Haas U. (1997) - Der Flimser Bergsturz, doch ein warmzeitliches Ereignis?. Bulletin für angewandte Geologie, 2(1), 35-46.

Weidinger J.T., Korup O., Munack H., Altenberger U., Dunning S.A., Tippelt G., Lottermoser W. (2014) - Giant rockslides from the inside. Earth and Planetary Science Letters, 389, 62-73.

Wood J.L., Harrison S., Reinhardt L. (2015) - Landslide inventories for climate impacts research in the European Alps. Geomorphology, 228, 398-408.

Zerathe S., Lebourg T., Braucher R., Bourlès D. (2014) - Mid-Holocene cluster of large-scale landslides revealed in the Southwestern Alps by ^{36}Cl dating. Insight on an Alpine-scale landslide activity. Quaternary Science Reviews, 90, 106-127

Ms. received: August 25, 2020 Revised: October 28, 2020
Accepted: December 2, 2020 Available online: December 20, 2020